

# Transactions Letters

## On the Capacity Formula for Multiple Input–Multiple Output Wireless Channels: A Geometric Interpretation

P. F. Driessen, *Senior Member, IEEE*, and G. J. Foschini

**Abstract**—The capacity of multiple input, multiple output (MIMO) wireless channels is computed for Ricean channels. The novelty is a geometrical (ray-tracing) interpretation of the MIMO channel capacity formula to find array geometries which greatly enhance channel capacity compared to single input–single output (SISO) systems.

**Index Terms**—Array signal processing, channel capacity, land mobile radio cellular systems.

### I. INTRODUCTION

A MULTIPLE input–multiple output (MIMO) wireless communications channel with a matrix transfer function of independent complex Gaussian random variables has an information-theoretic capacity which grows linearly with the number of antenna array elements  $n$ , for fixed power and bandwidth [1].

For line-of-sight (LOS) channels, we use ray tracing to construct a matrix transfer function (channel response) explicitly for some example environments and find array geometries which result in channel matrices with close to  $n$  nonnegligible eigenvalues, with corresponding high capacity. The LOS matrix channel response will change as the receiver is moved, so that a capacity distribution is obtained from the ensemble of sample matrix elements at different receiver locations. Also, a Rayleigh matrix may be added to the LOS channel matrix to form a matrix of Ricean scalars, from which a capacity distribution is obtained. In either case, we define an outage threshold  $x$  (say 0.01), and define  $C_x$  to be that capacity for which  $\text{Prob}\{C > C_x\} = 1 - x$ .

In what follows, the MIMO channel capacity formula is used to compute the capacity for three example geometries, plus one Ricean example, with a discussion of the results.

### II. CAPACITY CALCULATIONS AND ARRAY GEOMETRY

The capacity in b/s/Hz of a MIMO wireless system with  $n_T$  transmit antennas and  $n_R$  receive antennas with an average received SNR  $\rho$  (independent of  $n_T$ ) at each receive antenna

Paper approved by N. C. Beaulieu, the Editor for Wireless Communication Theory of the IEEE Communications Society. Manuscript received February 18, 1997; revised May 29, 1998; and August 11, 1998.

P. F. Driessen is with the Department of Electrical and Computer Engineering, University of Victoria, Victoria, BC V8W 3P6, Canada (e-mail: driessen@uvic.ca).

G. J. Foschini is with Bell Laboratories, Lucent Technologies, Holmdel, NJ 07733-0400 USA.

Publisher Item Identifier S 0090-6778(99)01929-7.

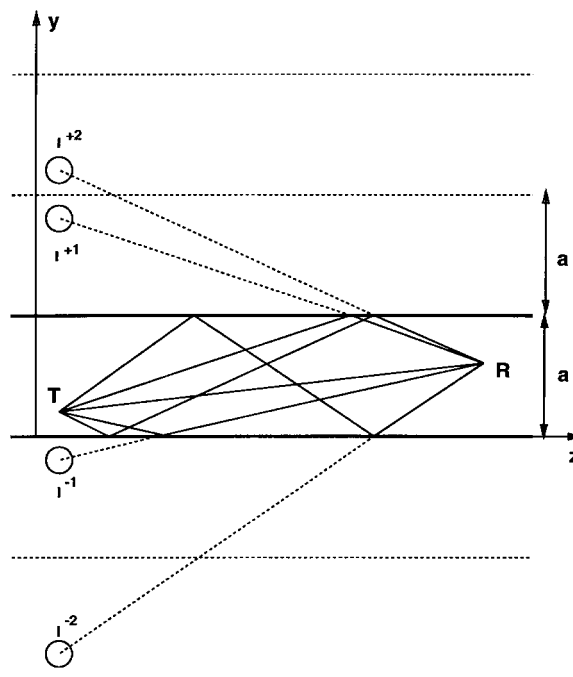


Fig. 1. Images in street canyon—top view  $a = 25$  m,  $\lambda = 1/3$  m,  $T(x, y, z) = (1, 15, 0)$  m,  $R(x, y, z) = (1, 5, 30)$  to  $(1, 6, 40)$ .

was obtained in [1] as  $C = \log_2(\det[I_{n_R} + (\rho/n_T)HH^*])$ , where the normalized channel matrix  $H$  contains complex scalars with unity average power loss, and  $H^*$  is the complex conjugate transpose of  $H$ . The capacity is expressed in b/s/Hz in the narrow-band limit with no frequency dependence. Normalization is achieved by dividing out the free space power loss and setting the parameter  $\rho$  to the desired SNR.<sup>1</sup> This result assumes that  $H$  is unknown to the receiver but  $n_R$  and  $\rho$  are known [1], [2]. The transmitted data has been demultiplexed into substreams which are separately independently coded and modulated on each antenna [6], so that the transmission from each antenna is different. The practicality of such MIMO wireless systems, using space-time coding with no bandwidth penalty, is illustrated in [3]–[5] and [7].

#### A. Line-of-Sight Channels

We first consider an environment with only free space nonfading LOS propagation and  $T$  and  $R$  arrays of  $n_T =$

<sup>1</sup>This avoids the need to compute absolute propagation loss and then select the transmitted power to obtain the desired SNR.

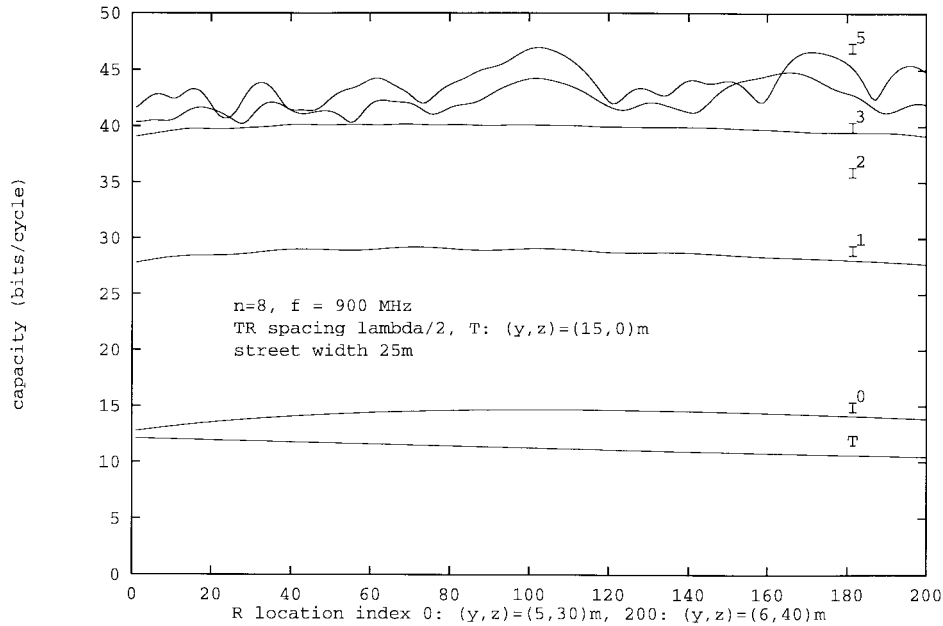


Fig. 2. Capacity versus  $R$  location in street canyon  $T$  and  $R$  height  $x = 1$  m,  $\rho = 20$  dB,  $\lambda = 1/3$  m.

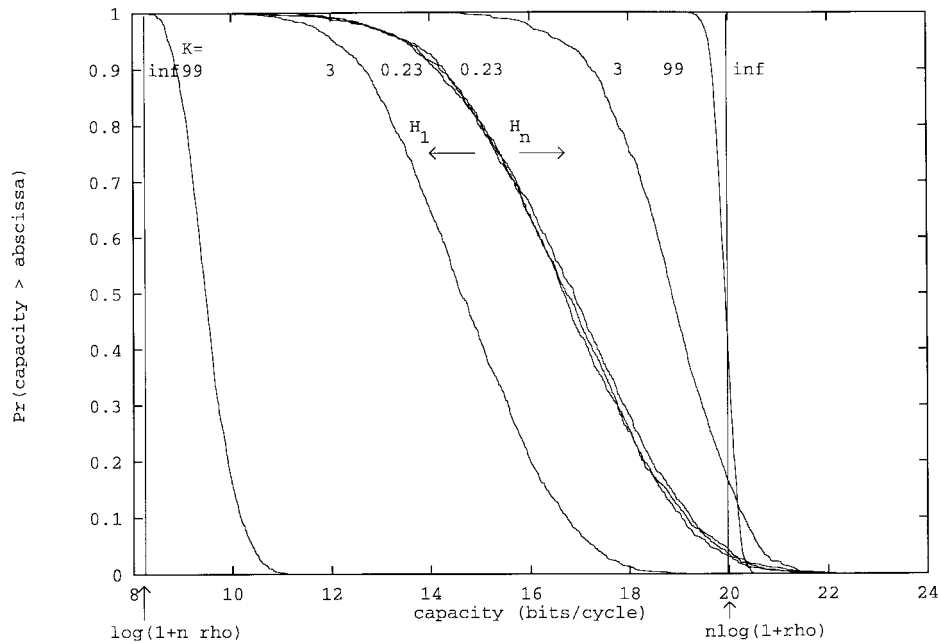


Fig. 3. Capacity on Ricean channels,  $n = 3$ .

$n_R = n$  antennas. The base and subscriber ends of the link are designated as  $T$  and  $R$ , respectively, but reciprocity applies. For LOS propagation, and a narrow-band channel at fixed carrier frequency  $f_c = c/\lambda$ , ray-tracing from  $T$  to  $R$  yields the channel transfer function matrix  $H = H_{\text{LOS}}$  with complex scalar entries

$$H_{ik} = |T_1 - R_1| \frac{\exp(-j2\pi|T_i - R_k|/\lambda)}{|T_i - R_k|} \quad (1)$$

where  $T_i, R_i$  are coordinate vectors for the  $i$ th element of

$T, R$ .  $H_{ik}$  is normalized by the distance between the reference locations  $T_1, R_1$ , so that  $H_{1,1} = 1$  and the absolute attenuation need not be calculated.

If the antennas are spaced less than  $\lambda/2$  apart at both  $T$  and  $R$ ,  $H_{ik} = e^{j\theta_{ik}} \simeq e^{j\theta}$  for fixed  $\theta$  for all  $i, k$ ,  $(HH^*)_{ik} \simeq n$ , and  $C = \log_2(1 + n\rho) = C_{\text{log}}$ , so that  $C_{\text{log}}$  increases logarithmically with  $n$ . For this case,  $H = H_{\text{LOS}} = H_1$  is of rank 1, and the capacity gain is essentially due to the  $n$ -fold array gain in  $\rho$ .

For arrays of  $n$  more widely spaced antennas at  $T$  and/or  $R$ , the complex scalars  $H_{ik}$  all have magnitude near one but different phases  $\theta_{ik}$ . For  $\theta_{ik}$  so that  $HH^* = nI_n$ ,  $H =$

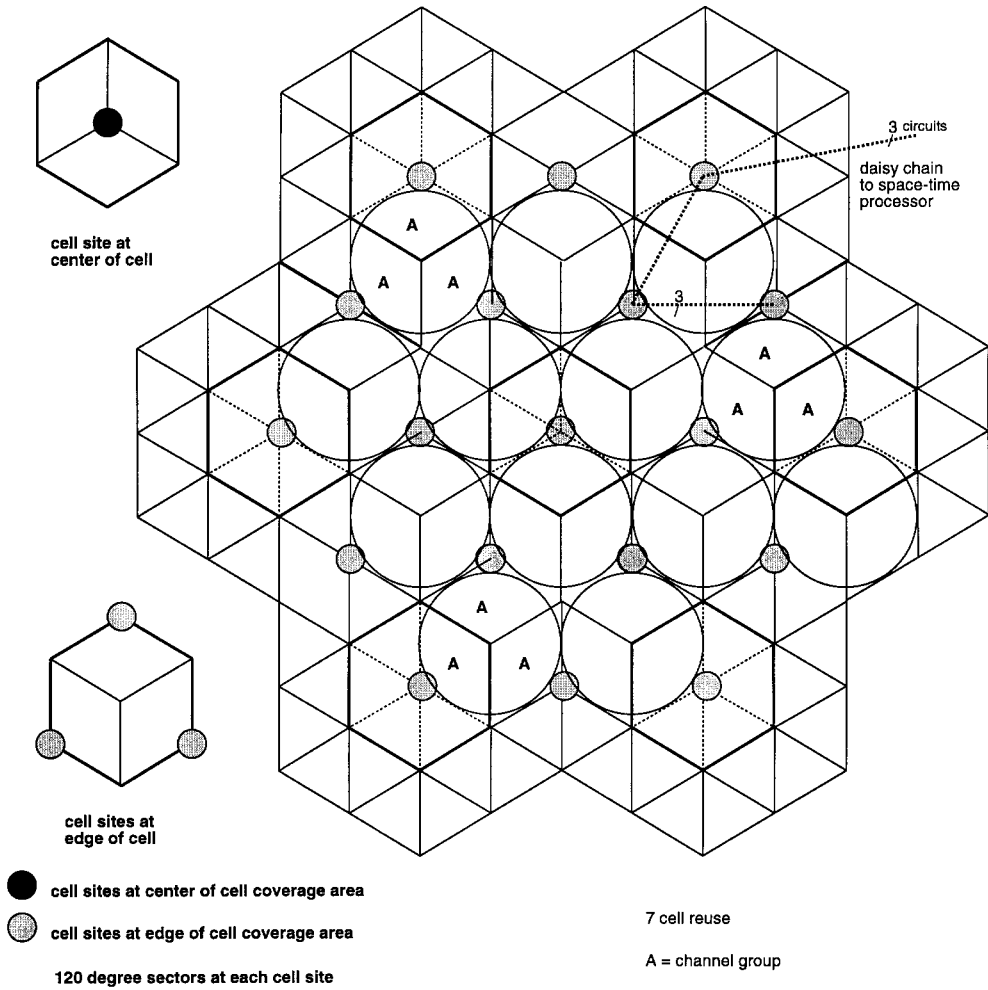


Fig. 4. Cell sites at center and edge of coverage area.

$H_{LOS} = H_n$  is of rank  $n$ , and  $C = n \log_2(1 + \rho) = C_{\text{lin}}$ , so that  $C_{\text{lin}}$  increases linearly with  $n$ . An example is  $\theta_{ik} = \frac{\pi}{n}[(i - i_0) - (k - k_0)]^2$  where for  $n = 2$  and  $i_0 = k_0 = 0$ ,  $H_{\text{max}} = \begin{pmatrix} 1 & j \\ j & 1 \end{pmatrix}$ , and the corresponding array geometry is two linear arrays broadside to each other. In what follows, we show three more examples of geometric arrangements for which  $H_{LOS} \simeq H_n$ .

One such arrangement is an  $n$ -element  $T$  array spread along an arc at angles  $\phi_{k-1}$  for  $k = 1, \dots, n$ , and a linear  $R$  array oriented broadside to the center of the arc. From (1), for arc radius  $D \gg \lambda$ , and interelement spacing  $z_r$ ,  $H_{ik} = \exp(j \frac{2\pi z_r}{\lambda} [(i-1) - \frac{n-1}{2}] \sin \phi_{k-1})$  which corresponds to the autocorrelation  $R_{xx}(i-k) = \frac{1}{2\Delta} \text{Re} \int_{-\Delta}^{\Delta} e^{j \frac{2\pi z_r}{\lambda} (i-k) \sin \beta} d\beta$  from [8, eq. (A-13)] specialized for the  $n$  discrete angles of arrival  $\phi_{k-1}$ .  $C \simeq C_{\text{lin}}$  when the angle subtended by the arc  $2\Delta = \phi_{n-1} - \phi_0$  is consistent with the beamwidth  $2\Delta = \lambda/z_r$  at which  $R_{xx}(i-k) = 0$ . The radiation pattern of the  $R$  array with all elements in phase  $E(\phi) = \frac{\sin(n\gamma/2)}{n \sin(\gamma/2)}$ , where  $\gamma = 2\pi z_r \sin \phi / \lambda$ . For  $z_r = \lambda/2$ , and the  $n$  array elements of  $T$  placed along the arc at  $\phi_{k-1}$  exactly in the nulls of  $R$ ,  $H_{ik} = \exp(j \frac{2\pi}{n} (i - i_0)(k - k_0))$  where  $i_0 = k_0 = \frac{n+1}{2}$ , for which  $HH^* = nI_n$  so that  $H = H_n$  and  $C = C_{\text{lin}}$ .

The second example arrangement is an  $n$ -element  $T$  array with elements spread evenly around a circle of radius  $D \gg \lambda$ ,

and a similar  $R$  array on a circle of radius  $D_r \leq \lambda$  at the center of the  $T$  array. From (1),  $H_{ik} = \exp(j \frac{2\pi D_r}{\lambda} \cos[(i-k) \frac{2\pi}{n}])$ . For  $D_r = \lambda/2$ , the  $T$  elements are not in the nulls of the  $R$  array, but the elements of  $HH^*$  for which  $i-k$  is odd are zero, and the off-diagonal even elements are approximately  $0.3n$ . Nonetheless, the capacity approaches  $C_{\text{lin}}$ , consistent with the observation [8] that small correlation ( $< 0.3$ ) has negligible effect on performance. Further calculations confirm that the capacity is robust in the presence of rotation or lateral movement of  $R$  or perturbations in the placement of the  $T$  elements.

The third example is an urban street geometry with two parallel reflectors representing the building walls separated by the street width  $a$  (Fig. 1).  $I^{\pm m}$  represents an image due to  $m$  specular reflections from the walls, and  $I^0$  is the "ground reflection" image not visible in the figure. For this street geometry, the elements of  $H$  may be written

$$\frac{H_{ik}}{|T_i - R_k|} = \frac{\exp(-j2\pi|T_i - R_k|/\lambda)}{|T_i - R_k|} + \sum_{k=-m}^m \Gamma^k \frac{\exp(-j2\pi|I_i^k - R_k|/\lambda)}{|I_i^k - R_k|} \quad (2)$$

where  $\Gamma$  is the amplitude reflection coefficient,<sup>2</sup>  $m$  is the maximum number of reflections considered, and we have assumed isotropic array elements.

For eight-element linear arrays with  $\lambda/2$  spacing oriented perpendicular to the street, Fig. 2 shows how the capacity increases as more images are added (and the angular spread of rays increases) and approaches  $C_{\text{lin}}$  with seven images ( $|m| \leq 3$ ) plus  $T$ . Furthermore, the received signal envelope looks increasingly Rayleigh-like as more images are added.

### B. Ricean Channels

Next we consider the capacity for Ricean channels, where the deterministic component  $H_{\text{LOS}}$  is fixed as either  $H_1$  or  $H_n$ . We follow the simulation methods of [1] using the normalized Ricean channel matrix  $H = (aH_{\text{LOS}} + bH_{\text{Rayleigh}})$  with  $a^2 + b^2 = 1$  and Ricean  $K$ -factor  $K = a^2/b^2$ . The results for  $n = 3$  with  $\rho = 100$  (20 dB) (Fig. 3) quantify how for closely spaced ( $\leq \lambda$ ) array elements at both  $T$  and  $R$ , and no reflectors or scatterers such that  $H_{\text{LOS}} \simeq H_1$ , the capacity decreases with increasing  $K$  toward  $C = C_{\text{log}}$ . However, for array geometries such as the above examples, where  $H_{\text{LOS}} \simeq H_n$ , the capacity increases with increasing  $K$  toward  $C = C_{\text{lin}}$ . For  $K = 0$ ,  $C$  corresponds to that obtained in [1].

### III. DISCUSSION

Capacities approaching  $C_{\text{lin}} = n \log_2(1+\rho)$  can be achieved for MIMO channels in an LOS (non-Rayleigh) environment by spreading out the elements of  $T$  either explicitly (by placing one element of  $T$  at each of  $n$  sites), or implicitly (by adding reflectors which create images of  $T$ ). The results of the second example suggest that three sectors in a conventional

<sup>2</sup>In general, the  $\Gamma$  are different for each image, since they depend on the angles of incidence and reflection, and the surface characteristics. Here we assume  $\Gamma$  has the same constant value 0.6 for all reflections, except the ground reflection  $\Gamma^0$  which is set to  $-1$ . This approximation is sufficient to illustrate the capacity gain.

cellular system can be combined to form one “edge-excited” (inward-facing) cell (Fig. 4) to enhance capacity for  $R$  not close to a base station. This is reminiscent of soft handoff in CDMA systems where multiple base stations serve one mobile, except that in this case, each base station carries a different substream of the transmitted data. The results of the third example suggest that in the absence of reflectors, we may use  $n$  antennas at each of  $n$  sites, thus replicating the effect of images of the  $n$ -element  $T$  array. The ray-tracing channel model for  $H = H_{\text{LOS}} + H_{\text{Rayleigh}}$  described here may be useful for the performance evaluation of MIMO wireless systems which use spatial diversity through space-time coding to exploit the available capacity with no bandwidth penalty (e.g. [2], [5]–[7]).

### REFERENCES

- [1] G. J. Foschini and M. J. Gans, “On limits of wireless communication in a fading environment when using multiple antennas,” *Wireless Personal Commun.*, vol. 6, no. 3, pp. 311–335, Mar. 1998.
- [2] G. J. Foschini, “Layered space-time architecture for wireless communication in a fading environment when using multi-element antennas,” *Bell Labs Tech. J.*, vol. 2, no. 2, pp. 41–59, Autumn 1996.
- [3] V. Weerackody, “Diversity for the direct-sequence spread spectrum system using multiple transmit antennas,” in *IEEE Int. Conf. Communications*, Geneva, Switzerland, May 1993, pp. 1775–1779.
- [4] N. Seshadri and J. H. Winters, “Two signalling schemes for improving the error performance of frequency-division-duplex (FDD) transmission systems using transmitter antenna diversity,” *Int. J. Wireless Information Networks*, vol. 1, no. 1, pp. 49–60, 1994.
- [5] D. Agrawal, V. Tarokh, A. Naguib, and N. Seshadri, “Space-time coded OFDM for high rate wireless communication over wideband channels,” in *Proc. IEEE Vehicular Technology Conf.*, 1998, pp. 2232–2236.
- [6] D. Agrawal, V. Tarokh, A. Naguib, N. Seshadri, and A. R. Calderbank, “Space-time codes for high data rate wireless communication: Performance criteria and code construction,” *IEEE Trans. Inform. Theory*, vol. 44, pp. 744–765, Mar. 1998.
- [7] D. Agrawal, V. Tarokh, A. Naguib, N. Seshadri, and A. R. Calderbank, “Space-time codes for high data rate wireless communication: Practical considerations,” *IEEE Trans. Commun.*, to be published.
- [8] J. Salz and J. H. Winters, “Effect of fading correlation on adaptive arrays in digital mobile radio,” *IEEE Trans. Veh. Technol.*, vol. 43, pp. 1049–1057, Nov. 1994.